Supplementary Information

Table S1. High grade ovarian serous cancer patient characteristics

		Overall survival			DFI		
		N (%)	P	HR (95%CI)	N (%)	P	HR (95%CI)
Age mean (min-max)		212 58 (22-84)	0.0006	1.03 (1.0,1.1)	208 58 (22-84)	0.0036	1.02 (1.0, 1.0)
Stage	I, II	44 (21%)	0.0014	3.2 (1.7, 7,2)	43 (21%)	0.0002	3.78 (2.0, 8.1)
	III, IV	168 (79%)			165 (79%)		
Debulking	Optimal	116 (55%)	<0.0001	0.46 (0.3, 0.7)	114 (56%)	<0.0001	0.46 (0.3, 0.7)
	Suboptimal	94 (45%)			91 (44%)		

Note: Optimal debulking is defined as residual implants ≤ 1 cm. DFI, disease-free interval.

Table S1, related to Figure 2

Table S2. Cancer patient characteristics

		miR101		CD33		CtBP2	
		Low	High	Low	High	Low	High
Age mean (min-max)		56 (22-80)	59 (41-78)	55 (22-84)	58 (30-80)	54 (22-78)	56 (30-84)
Stage	I, II	28%	21%	29%	8%	16%	26%
	III, IV	72%	79%	71%	92%	84%	74%
Debulking	Optimal	63%	54%	63%	73%	68%	66%
	Suboptimal	37%	46%	37%	27%	32%	34%

Note: Optimal debulking is defined as residual implants ≤ 1 cm. DFI, disease-free interval.

Table S2, related to Figure 2, 5, 7

Table S3. MicroRNA arrays (excel file)

Note: Effects of MDSCs on microRNA profile in primary ovarian cancer cells. Primary ovarian cancer cells were co-cultured with MDSCs or blood $lin^-CD45^+CD33^+$ cells or medium for 24 hours, and were subsequently subject to a quantitative PCR microRNA array. The expression of microRNAs was presented as the relative expression to U6. Red spot shows microRNA101. Set 1: Array 1 (medium) and array 2 (MDSCs). Set 2: array 3 (medium), array 4 (MDSCs) and array 5 (blood $lin^-CD45^+CD33^+$).

Table S3, related to Figure 4

Table S4. ChIP primers

ChIP-OCT4/3-F	AGCCGCTGGCTTATAGAAGGTGC;
ChIP-OCT4/3-R	CCAGCTTGCTTTGAGGGTCCCA
ChIP-NANOG-F	CGCCAGGAGGGGTGGGTCTAA;
ChIP-NANOG-R	GCAAGCTTTGGGGACAAGCTGGA
ChIP-SOX2-F	TCCCTGACAGCCCCCGTCAC;
ChIP-SOX2-R	TGCCGCCGCCGATGATTGTT

Table S4, related to Method

Supplementary figure legends:

Figure S1, CD33 expression and MDSCs.

(A, B) Phenotype of MDSCs. Single cell suspension was made from fresh ovarian cancer tissues. Cells were stained with specific antibodies against human MHC-II (HLA-DR), human endothelial/progenitor cells (CD34), T cells (CD3), B cells (CD19) and NK cells (CD16, CD56), leukocytes (CD45), neutrophils (CD15, CD16) and epithelial cells (epithelial cell adhesion molecule, EpCAM). Polychromatic flow cytometry analysis demonstrated that $lin^-CD45^+CD33^+$ cells infiltrated ovarian cancer. (A) The relationship between CD15, CD16, HLA-DR and CD33 is shown in ovarian cancer. (B) When $CD33^+$ cells were gated from original single cells, $CD33^+$ cells were confined to lin^-CD45^+ cells in ovarian cancer. When $CD33^-$ cells were gated from original single cells, $CD33^-$ but not $CD33^+$ cells were confined to T cells, B cells, NK cells and $CD34^+$ cells in ovarian cancer. One of 12 is shown.

(C) Phenotype of blood $lin^-CD45^+CD33^+$ cells. Phenotype of blood $lin^-CD45^+CD33^+$ cells was analyzed with FACS. Arrow indicated blood $CD33^+$ myeloid cells. One of 8 is shown.

(D) Effects of blood $lin^-CD45^+CD33^+$ cells on T cell proliferation in vitro. Autologous T cells were cultured with blood $lin^-CD45^+CD33^+$ cells with different ratios for 3 days. T cell proliferation was determined by thymidine incorporation. $n = 5$, $P > 0.05$, as compared to controls.

(E) Effects of tumor associated MDSCs on tumor growth in vivo. Autologous TAA-specific T cells were conditioned with MDSCs and injected into NSG mice bearing established ovarian cancer. Results are shown as the mean tumor volume ± SEM. Tumor cells and T cells were from two patients (C). $n = 4$/group. $P < 0.01$, as compared to no MDSC and controls (Day 9 and 12).

Figure S1, related to Figure 1

Figure S2, $CD33^+$ cells in ovarian cancer.

One staining example in high magnification with a portion of whole core. Ovarian cancer tissues were stained with anti-CD33 antibody. The density of $CD33^+$ cells was quantified. Figure S2, related to Figure 2

Figure S3, Effects of MDSCs on ovarian cancer incidence and growth

(A, B) Effects of MDSCs on ovarian cancer incidence and growth. Primary ovarian cancer cells were conditioned with MDSCs and inoculated into NSG mice. Ovarian cancer growth (A) and incidence (B) were recorded. (A) Primary ovarian cancer cells (200,000/mouse) were subcutaneously injected into NSG mice Results are expressed as the mean tumor volume ± SD, n = 4-6/group, $P > 0.05$. (B) 1000-200,000 cells were injected into NSG mice. One of 3 independent experiments

(C, D) Effects of MDSCs on ovarian cancer lung metastasis. Primary ovarian cancer cells were co-cultured with MDSCs for 48 hours, and subsequently were intravenously injected into NSG mice (50,000 cells/mouse). Liver metastatic foci were counted at day 50 after tumor inoculation. Results are shown as the mean ± SEM (C). 5 mice/group in two independent experiments. $P < 0.05$. Liver tumor foci are shown (D).

(E) Effect of blood $lin^-CD45^+CD33^+$ cells on tumor incidence. Blood $lin^-CD45^+CD33^+$ cells-conditioned primary ovarian cancer cells were subcutaneously injected into NSG mice. Tumor development was monitored. Results are expressed as the percentage of tumor development. n = 4/group. $P > 0.05$.

(F) Effect of blood $lin^-CD45^+CD33^+$ cells on stemness associated gene expression. Tumor stem cell associated gene transcripts were quantified with real-time PCR and are expressed as the mean values relative to controls ± SD. Three experiments with triplicates, $P > 0.05$.

(G) Effect of blood $lin^-CD45^+CD33^+$ cells on sphere formation. Primary ovarian cancer cells were cultured with blood $lin^-CD45^+CD33^+$ cells. Sphere assay was performed. 2 donors with triplicates. $P > 0.05$.

Figure S3, related to Figure 3

Figure S4. Effects of MDSCs on tumor microRNA profile.

(A) Effects of MDSCs on microRNA profile in primary ovarian cancer cells. Primary ovarian cancer cells were co-cultured with MDSCs for 24 hours, and were subsequently subject to a quantitative PCR microRNA array. The expression of microRNAs was presented as the relative expression to U6. Red spot shows microRNA101. One of 3 is shown.

(B) Effects of MDSCs on microRNA145, 155 and 200 in primary ovarian cancer cells. Primary ovarian cancer cells were cultured with MDSCs. The expression of microRNA145, microRNA155 and microRNA200 was quantified by real-time PCR in MDSC-conditioned and control primary ovarian cancer cells. Results are expressed as the relative expression to U6 ± SD. n = 4 with triplicates. $P > 0.05$.

Figure S4, related to Figure 4

Figure S5, Expression of microRNA101 in secondary sphere formation and effect of micorRNA101 on ovarian cancer cell proliferation.

(A) Expression of microRNA101 on secondary sphere formation. Primary sphere forming ovarian cancer cells were subject to secondary sphere formation assay. The expression of microRNA101 was quantified by real-time PCR in secondary sphere forming ovarian cancer cells and parental cells. Results are expressed as the relative expression to U6 ± SD. n = 3 with triplicates. *, $P < 0.05$.

(B) Effect of micorRNA101 on ovarian cancer cell proliferation. Parental, stable microRNA101 and vector expressing primary ovarian cancer cells were cultured for 16

hours. Thymidine incorporation was measured at the last 6 hours. Results are expressed as the mean of CPM values ± SEM. Three experiments with triplicates. $P > 0.05$.
Figure S5, related to Figure 5

Figure S6, Effect of microRNA101 knockdown on PRC2 expression and relationship between CtBP2 and ovarian cancer cell proliferation/growth.
(A) Effect of microRNA101 knockdown on PRC2 expression. Stable microRNA101 and vector expressing primary ovarian cancer cells were subject to detect PRC2 members, Ezh2, Suz12 and EED expression with Western blot. One of 3 experiments is shown.

(B) Effect of CtBP2 on ovarian cancer cell proliferation. Parental, stable sh-CtBP2 and vector expressing primary ovarian cancer cells were cultured for 16 hours. Thymidine incorporation was measured at the last 6 hours. Results are expressed as the mean of CPM values ± SEM. Three experiments with triplicates. $P > 0.05$.

(C) Effect of CtBP2 on ovarian cancer growth. Stable sh-CtBP2 and vector expressing primary ovarian cancer cells were subcutaneously injected into NSG mice. Tumor volume was monitored. Results are expressed as the mean of tumor volume ± SEM. N = 5/group. $P > 0.05$.
Figure S6, related to Figure 6

Figure S7, $CtBP2^+$ ovarian cancer cells. Ovarian cancer tissues were stained with anti-CtBP2 antibody. $CtBP2^+$ tumor cells were quantified with the H-score as we described in Methods. < the median values were considered low CtBP2 expression, and ≥ the median values were considered high CtBP2 expression.

(A, B) One staining example for low CtBP2 expression, in low magnification with whole core (A) and high magnification with a portion of whole core (B).

(C, D) One staining example for high CtBP2 expression, in low magnification with whole core (C) and high magnification with a portion of whole core (D).

Figure S7, related to Figure 7

Supplementary Method:

MDSCs mediated TAA-specific T cell immunosuppression in vivo

We used established TAA-specific T cells for the in vivo immune suppression experiments. To establish TAA-specific T cells, HLA-$A2^+$ $Her2/neu^+$ ovarian cancer patients were selected for this study. Autologous ovarian cancer ascites $CD25^-$ T cells were stimulated with anti-CD3, anti-CD28 and monocytes loaded with three distinct HLA-A2-binding Her-2/neu peptides at 5 μg/ml each: p369-384 (KIFGSLAFLPESFDGDPA), p688-703 (RRLLQETELVEPLTPS), and p971-984 (ELVSEFSRMARDPQ) (Multiple Peptide System, Seattle, WA), as we described (Curiel et al., 2004; Curiel et al., 2003; Kryczek et al., 2006). Primary ovarian tumor cells (1×10^7) in 200 μl of buffered saline were subcutaneously injected into dorsal tissues of female NSG mice (6-8 weeks old, Jackson Lab, Bar Harbor, Maine). Autologous TAA-specific T cells (6×10^6) were conditioned with MDSCs (3×10^6) or medium, and were subsequently injected intravenously into mice on day 12 after human tumor inoculation (Curiel et al., 2004; Curiel et al., 2003; Kryczek et al., 2006). The viability of the injected T cells was > 95%. Tumor size was measured using calipers fitted with a Vernier scale. Tumor volume was calculated based on three perpendicular measurements.

Figure 1S

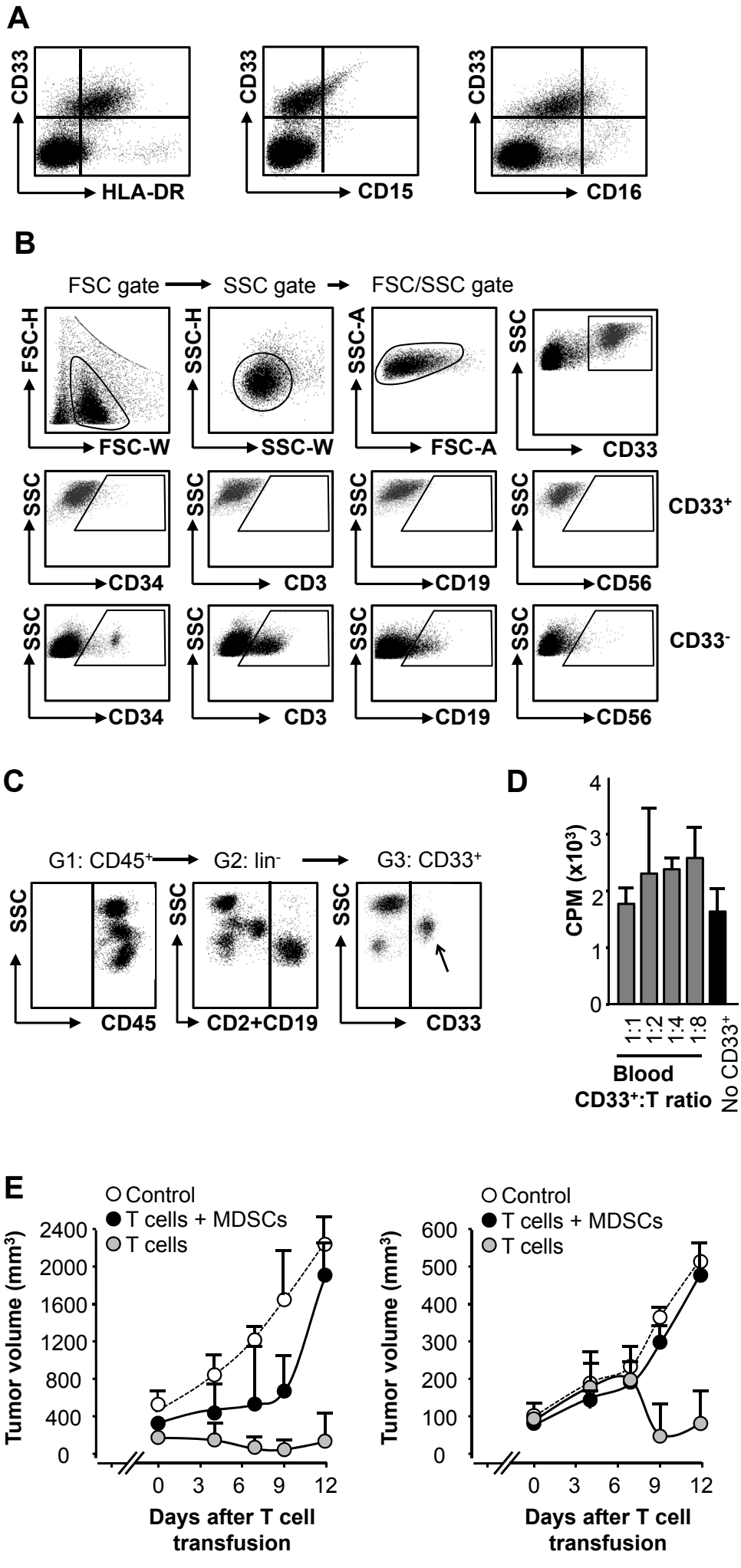
A
CD33
HLA-DR
CD33
CD15
CD33
CD16
B
FSC gate
SSC gate
FSC/SSC gate
FSC-H
FSC-W
SSC-H
SSC-W
SSC-A
FSC-A
SSC
CD33
SSC
CD34
CD3
CD19
CD56
CD33+
CD33-
C
G1: CD45+
G2: lin-
G3: CD33+
SSC
CD45
CD2+CD19
CD33
D
CPM (x10³)
0
1
2
3
4
1:1
1:2
1:4
1:8
No CD33+
Blood
CD33+:T ratio
E
Control
T cells + MDSCs
T cells
Tumor volume (mm³)
2400
2000
1600
1200
800
400
0
0
3
6
9
12
Days after T cell transfusion
Control
T cells + MDSCs
T cells
Tumor volume (mm³)
600
500
400
300
200
100
0
0
3
6
9
12
Days after T cell transfusion

Figure 2

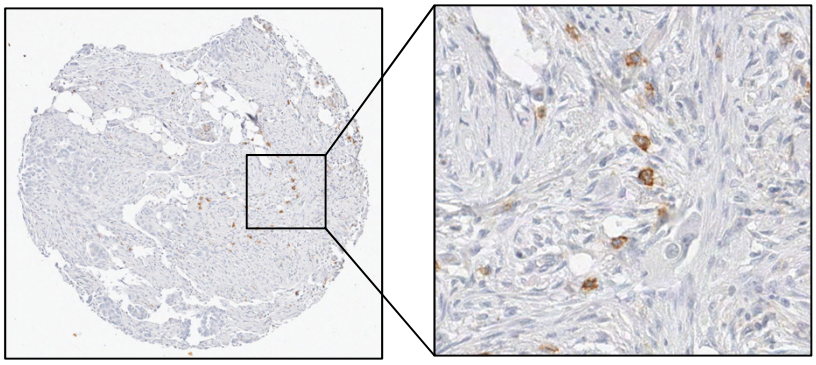

Figure 3S

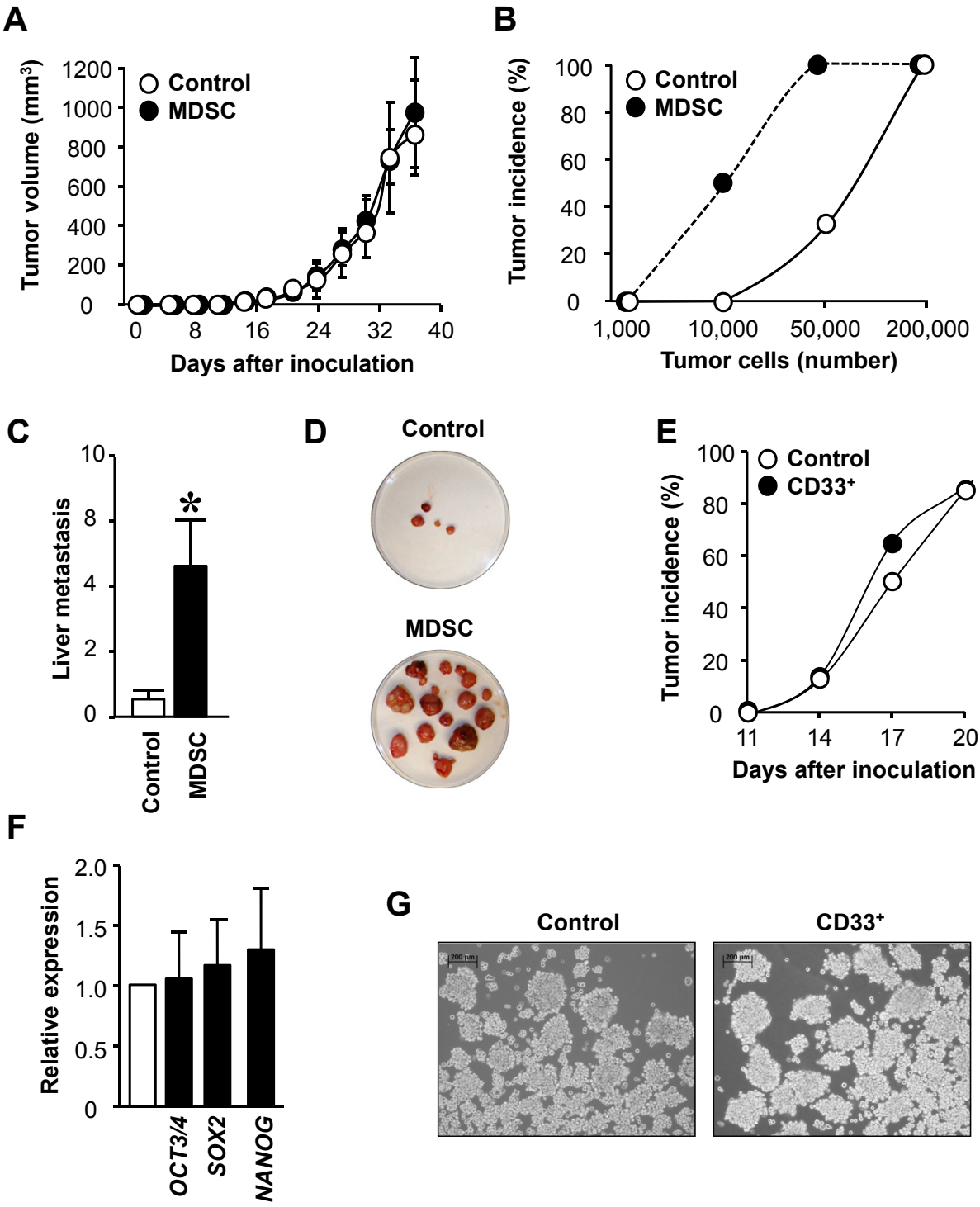
A
Tumor volume (mm³)
1200
1000
800
600
400
200
0
Control
MDSC
0
8
16
24
32
40
Days after inoculation
B
Tumor incidence (%)
100
80
60
40
20
0
Control
MDSC
1,000
10,000
50,000
200,000
Tumor cells (number)
C
Liver metastasis
10
8
4
2
0
*
Control
MDSC
D
Control
MDSC
E
Tumor incidence (%)
100
80
60
40
20
0
Control
CD33+
11
14
17
20
Days after inoculation
F
Relative expression
2.0
1.5
1.0
0.5
0
OCT3/4
SOX2
NANOG
G
Control
CD33+

Figure 4S

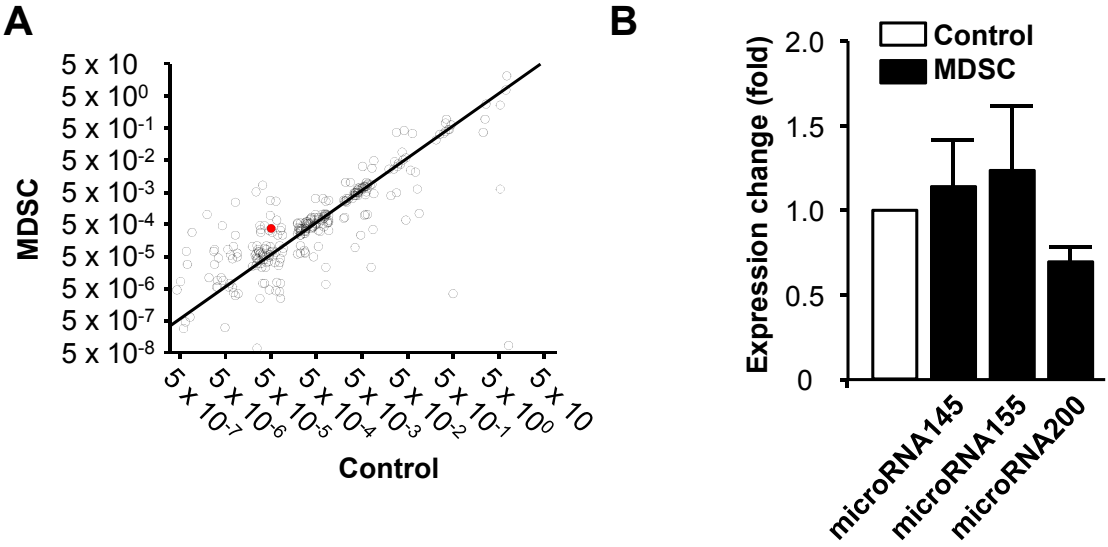
A
MDSC
Control
B
Control
MDSC
Expression change (fold)
2.0
1.5
1.0
0.5
0
microRNA145
microRNA155
microRNA200

Figure 5S

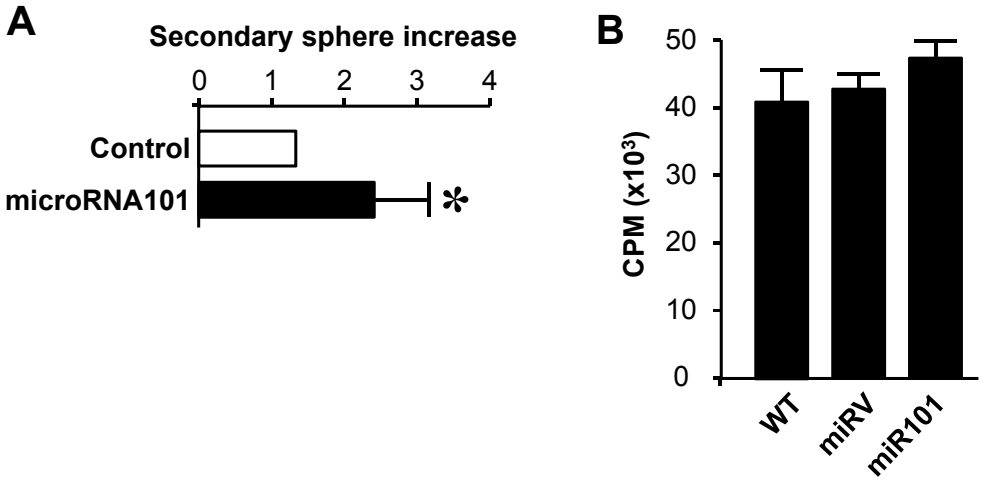
A
Secondary sphere increase
0
1
2
3
4
Control
microRNA101
*
B
50
40
30
20
10
0
CPM (x10³)
WT
miRV
miR101

Figure 6S

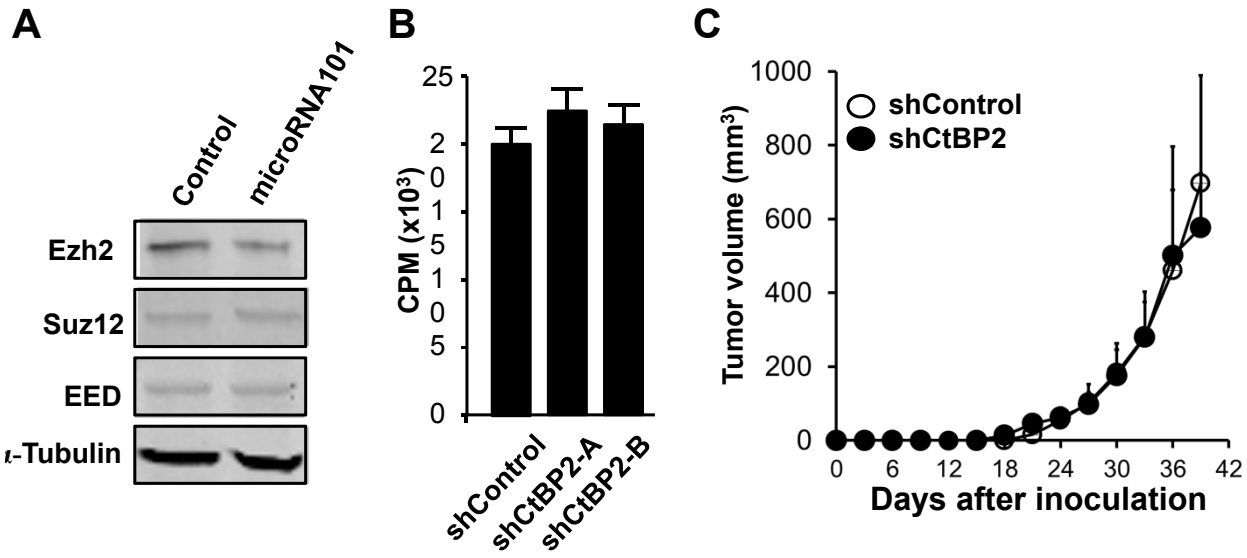
A
Control
microRNA101
Ezh2
Suz12
EED
α-Tubulin
B
CPM (x10³)
25
20
15
10
5
0
shControl
shCtBP2-A
shCtBP2-B
C
Tumor volume (mm³)
1000
800
600
400
200
0
shControl
shCtBP2
0
6
12
18
24
30
36
42
Days after inoculation

Figure 7S

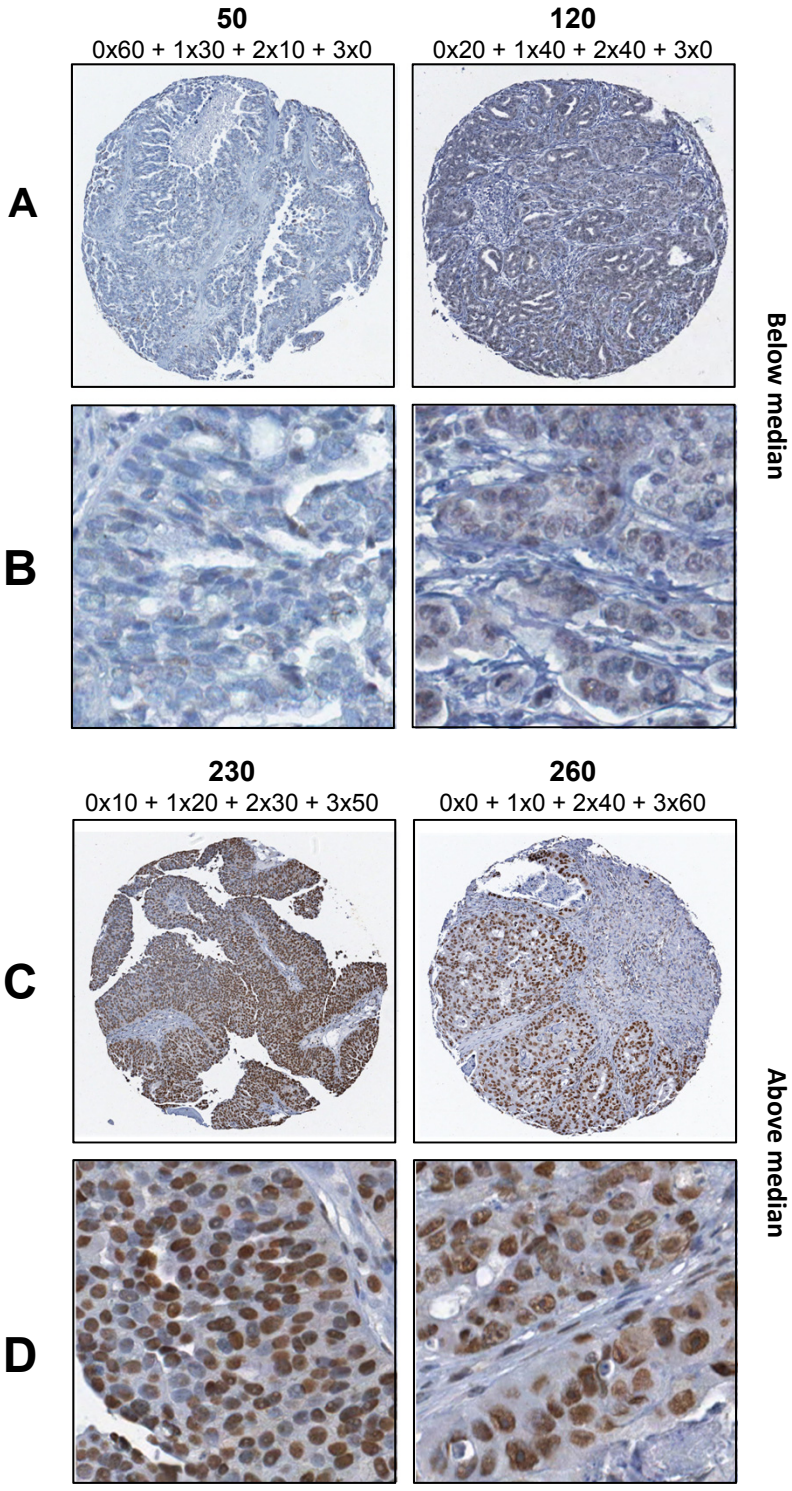
50
0x60 + 1x30 + 2x10 + 3x0
120
0x20 + 1x40 + 2x40 + 3x0
A
B
Below median
230
0x10 + 1x20 + 2x30 + 3x50
260
0x0 + 1x0 + 2x40 + 3x60
C
D
Above median